

# Temperature dependent Rolletti stability analysis of GaN HEMT

R. YILDIRIM, H. GÜÇLÜ YAVUZCAN, F. V. ÇELEBİ<sup>a\*</sup>, L. GOKREM<sup>b</sup>

Gazi Üniversitesi, Endüstriyel Sanatlar Eğt. Fak Gölbaşı-Ankara, Turkey

<sup>a</sup>Ankara Üniversitesi, Bilgisayar Müh. Böl., Beşevler-Ankara, Turkey

<sup>b</sup>Gaziosmanpaşa Üniversitesi, Meslek Yüksek Okulu- Tokat, Turkey

In this study, Rolletti stability criterion (K) analysis is performed based on the scattering parameters of GaN based High Electron Mobility Transistor (HEMT). The change in K and  $\Delta$  (Delta, D) with temperature is analyzed and the relationship between K and  $\Delta$  is determined. The frequency region where the effective temperature change is determined by indicating the critical points for the stability of HEMT. In addition to that, best values of K and  $\Delta$  are specified along with the boundary values and the region where HEMT works stable is determined.

(Received March 12, 2009; accepted July 20, 2009)

**Keywords:** HEMT, Stability, Rolletti, Temperature, GaN HEMT

## 1. Introduction

HEMT is a kind of Field Effect Transistor that is recently invented and finally commercialized [1]. HEMTs are commonly used in various areas due to their low noise and their ability to work at high frequencies. The working frequency of HEMTs, due to the material used, ranges between 10–110 GHz [1–27]. The main usage areas of HEMTs are; analog, numerical and wireless communication systems.

In this study, a GaN based HEMT is analyzed based on the temperature dependent scattering parameters, changes in power and gain. The cut-off frequency of the analyzed GaN-HEMT is 101 GHz, its maximum oscillation frequency is 155 GHz and its other properties are listed in references [28–29]. In the study, analyses are performed for scattering (S) and gain parameters of GaN HEMT at different Kelvin (K) temperatures (100 K, 200 K, 300 K, 400 K, 500 K and 600 K). There are different approaches related with the stability of HEMTs[30–35]. In this study, the relationship between Rolletti stability factor (K) and temperature is determined.

## 2. Hemt analysis

There are many equivalent circuit models proposed for HEMTs. The main ones are; high and low frequency, large and small signal equivalent circuits. That's why prior to making the circuit analysis, the equivalent circuit model suited to the purpose is selected [11–24]. Fig. 1 shows the equivalent circuit model for the chosen HEMT.

HEMT equivalent circuit model are analyzed in two groups as intrinsic and extrinsic elements. Extrinsic elements are  $L_g, L_s, L_d, R_g, R_s$  and  $R_d$ . whereas intrinsic elements are defined as gate charging

resistance  $R_i$ , gate-source conductance or resistance ( $g_{ds}, R_{ds}$ ), gate-source capacitance  $C_{gs}$ , dependent source  $G_m = g_m V_{gs}$ , gate-drain capacitance  $C_{gd}$ , drain-source capacitance  $C_{ds}$  and transconductance  $g_m$  [4].

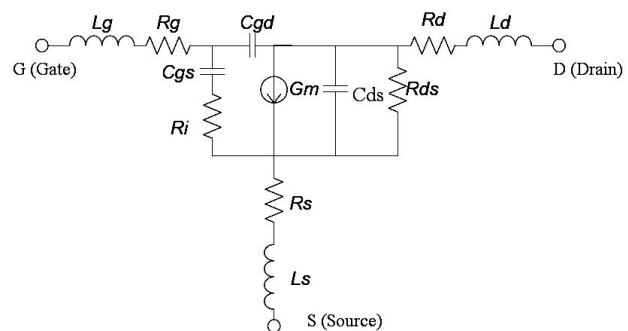


Fig. 1. HEMT small signal equivalent circuit model [6,7].

Equivalent circuit parameters are obtained by using two-port analysis techniques just like the ones used for scattering S, admittance Y, hybrid H and impedance Z parameters [8–25].

Whereas S parameters are defined as:

$S_{11}$ : The input reflection coefficient.

$S_{12}$ : The reverse transmission coefficient (reverse gain or loss).

$S_{21}$ : The forward transmission coefficient (forward gain).

$S_{22}$ : The output reflection coefficient. Table 1 shows the change with temperature of the equivalent circuit elements given in Fig. 1.

The non-linear output current of HEMT is defined as in [35]:

$$i_d(v_g, v_d) = \frac{\partial I_d}{\partial V_g} v_g + \frac{\partial I_d}{\partial V_d} v_d + \frac{1}{2} \frac{\partial^2 I_d}{\partial V_g^2} v_g^2 + \frac{1}{2} \frac{\partial^2 I_d}{\partial V_g \partial V_d} v_g v_d + \frac{1}{6} \frac{\partial^3 I_d}{\partial V_g^3} v_g^3 + \frac{1}{2} \frac{\partial^3 I_d}{\partial V_g^2 \partial V_d} v_g^2 v_d + \frac{1}{6} \frac{\partial^3 I_d}{\partial V_d^3} v_d^3 + \frac{1}{2} \frac{\partial^3 I_d}{\partial V_d^2 \partial V_g} v_d^2 v_g \quad (1)$$

where the trans-conductance is defined as  $g_m = g_{m1} + g_{m2} v_{gs} + g_{m3} v_{gs}^2$ . The  $g_{m1}$ ,  $g_{m2}$  and  $g_{m3}$  terms in this relation decrease respectively at the ratio of 19.579%, 25.327% and 50.119%. As a result, the output current decreases and this directly affects the gain. Whereas the output resistance (drain-source) is defined as  $r_{ds} = r_{ds1} + r_{ds2} v_{gs} + r_{ds3} v_{gs}^2$ . The output resistance change increases at the ratio of 263.004%, 222.655% and 185.259% for  $r_{ds1}$ ,  $r_{ds2}$  and  $r_{ds3}$  values respectively. The gate-source capacitance change is defined as  $C_{gs} = C_{gs1} + C_{gs2} v_{gs} + C_{gs3} v_{gs}^2$ . For  $C_{gs1}$ ,  $C_{gs2}$  and  $C_{gs3}$  the change ratios increase at 166.747%, 232.005% and 154.850% respectively. As a result of this, the working frequency of HEMT changes.

Table 1. Circuit parameters [28–29] at different temperatures of HEMT (Kelvin, K).

Parameter	T=100K	T=200K	T=300K	T=400K	T=500K	T=600K
$C_{gs1}$ (pF)	0.5795	0.6226	0.6754	0.7309	0.8191	0.9663
$C_{gs2}$ (pF/V)	-0.1581	-0.1814	-0.2086	-0.2315	-0.28	-0.3668
$C_{gs3}$ (pF/V <sup>2</sup> )	0.0567	0.0565	0.0573	0.0567	0.0653	0.0878
$g_{m1}$ (mS/mm)	263.75	221.79	177.33	133.73	89.488	51.64
$g_{m2}$ (mS/mm/V)	275.46	244.63	206.74	163.72	115.68	69.768
$g_{m3}$ (mS/mm/V <sup>2</sup> )	-49.085	-32.556	-14.5	2.7313	18.302	24.601
$r_{ds1}$ (k $\Omega$ )	395.1	491.992	450.457	588.175	851.343	1000
$r_{ds2}$ (k $\Omega$ /V)	-316.772	-398.615	-322.077	-421.463	-616.74	-705.210
$r_{ds3}$ (k $\Omega$ /V <sup>2</sup> )	84.249	104.863	77.955	100.664	146.691	156.079
$C_{gd}$ (pF)	0.07	0.07	0.07	0.07	0.07	0.07
$C_{ds}$ (pF)	0.05	0.05	0.05	0.05	0.05	0.05
$R_d$ ( $\Omega$ )	2.5	2.5	2.5	2.5	2.5	2.5
$R_i$ ( $\Omega$ )	1	1	1	1	1	1
$R_s$ ( $\Omega$ )	1.7	1.7	1.7	1.7	1.7	1.7

Transfer function is often used in system analysis. When maximum power transfer is required, signal power is usually taken as the variable parameter.

In a two-port system, the load impedance ( $Z_L$ ) is characterized by the scattering matrices [S] and chain matrix [ABCD]. The transducer power gain ( $g_T$ ); is the ratio of the power delivered to load ( $P_L$ ), to the power available from the source ( $P_{AVS}$ ). The transducer power gain is defined as;

$$g_T = \frac{P_L}{P_{AVS}} = \frac{|S_{21}|^2 (1 - |\Gamma_L|^2) (1 - |\Gamma_S|^2)}{|1 - \Gamma_{IN} \Gamma_S|^2 |1 - S_{22} \Gamma_L|^2} \quad (2)$$

where  $\Gamma_{IN}$  is the input reflection coefficient,  $\Gamma_{OUT}$  is the output reflection coefficient,  $\Gamma_L$  is the load reflection coefficient and  $\Gamma_S$  is the source reflection coefficient.

The transducer power gain depends on both the load and the source impedance. The available power gain ( $G_A$ )

depends on the ratio of the available power in a two-port ( $P_{AVN}$ ) to the available power at the source ( $P_{AVS}$ ). The available power gain relation  $G_A$  is defined as

$$G_A = \frac{P_{AVN}}{P_{AVS}} = \frac{1 - |\Gamma_S|^2}{|1 - S_{11} \Gamma_S|^2} |S_{21}|^2 \frac{1}{1 - |\Gamma_{OUT}|^2} \quad (3)$$

The relationship between transducer power gain and voltage gain relative to source signal voltage  $V_S$  and output voltage  $V_0$  which is given as,

$$V_g^2 = \frac{V_0^2}{V_S^2} = \frac{V_0^2 / R_L}{V_S^2 / 4R_S} \frac{R_L}{4R_S} = g_T \frac{R_L}{4R_S} \quad (4)$$

in which the load resistance ( $R_L$ ) and source series resistance ( $R_S$ ) are defined as in [30,33,34].

Stability in systems is defined as the bounded output with bounded input. There are many criteria for stability

analysis. These are Nyquist, Root-locus, Hurwitz, Rolletti, Linvilli and Stern etc. Some of these can be used for the analysis of control systems as well. There are different criteria for non-linear systems as well. These are Lyapunov I-II and Point care etc.

Even though there are many theoretical advantages of stability criteria, the results in practical applications are very limited. The design of high order non-linear systems can be given as a practical application example in [30–34].

In stability analysis, the input and output reflection coefficients of HEMT ( $\Gamma_{IN}, \Gamma_{OUT}$ ) are considered. The stability of HEMT has been related to both of these values being low [30]. In two-port systems when these two values are both low, the system is accepted to be stable [3, 31]. The instability condition occurs when both these values are high. The stability relations have been defined as [30, 32, 33]:

$$|\Gamma_{IN}| = \left| S_{11} + \frac{S_{12}S_{21}\Gamma_L}{1 - S_{22}\Gamma_L} \right| < 1 \quad |\Gamma_{OUT}| = \left| S_{22} + \frac{S_{12}S_{21}\Gamma_S}{1 - S_{11}\Gamma_S} \right| < 1 \quad (5)$$

If the Rolletti’s condition has been fulfilled, the stability factor  $K > 1$ , the circuit is accepted to be unconditionally stable [32–33]. Accordingly;

$$K = \frac{1 - |S_{11}|^2 - |S_{22}|^2 + |\Delta|^2}{2|S_{21}S_{12}|} > 1, \quad \Delta = S_{11}S_{22} - S_{12}S_{21} < 1 \quad (6)$$

$\Delta$  (Delta) values are calculated by using the S-parameters of HEMT and then the Rolletti stability factor  $K$  is calculated [32]. If  $K > 1$ , it is accepted to be unconditionally stable otherwise it can be potentially unstable ( $K < 1$ ) and most probably in many situations there is a discrepancy between the load impedance and the source.

The curves in Fig. 2 have been obtained by using the HEMT equivalent circuit in Fig. 1 and the values in Table 1. In the modeling, Rolletti stability factor ( $K$ ) and Delta ( $\Delta$ ) values have been obtained for different temperatures in 10MHz-500GHz frequency range.

At different temperatures an inverse relation has been determined between  $\Delta$  and  $K$  until HEMT became fully stable. In low frequencies (10-400 MHz),  $\Delta$  is at its maximum whereas  $K$  is at its minimum value. This holds for all the temperatures used in the test but it can be accepted that the frequencies after 1 GHz temperature dependent breakups occur between Delta and the Rollet stability factor. 16 GHz frequency is the point where the stability factor is at its maximum and Delta is at its minimum value. At this frequency the stability factor is  $K=1.21$  (at 600K temperature), Delta  $\Delta=0.02$  (at 400K temperature). Whereas the Rolletti factor value at which HEMT is unconditionally stable ranges between 36-93 GHz at different temperatures. After 300 GHz, the  $K$  and  $\Delta$  values approach to “1” for all temperatures used for testing. However this frequency is higher than the cut-off frequency (150 GHz) for the HEMT used. Theoretically, at all temperatures the system is stable for frequencies higher than 93 GHz. The steady state frequency range for the Rolletti stability factor value is between 12-93GHz interval. The frequency border values for which the Rolletti criteria do not go down to less than 1 are determined to be respectively 36GHz for 600K, 50GHz for 500K, 65GHz for 400K, 75GHz for 300K, 82GHz for 200K and 93GHz for 100K. The delta values reach to “1” for all temperatures after 300GHz. The stable region that can be used ideally for HEMT is between 75-150GHz for 300K which corresponds to room temperature. As a result, the stability is directly proportional to temperature of HEMTs which means that at higher temperatures the HEMT becomes stable at lower frequencies whereas for lower temperatures it becomes stable at higher frequencies.

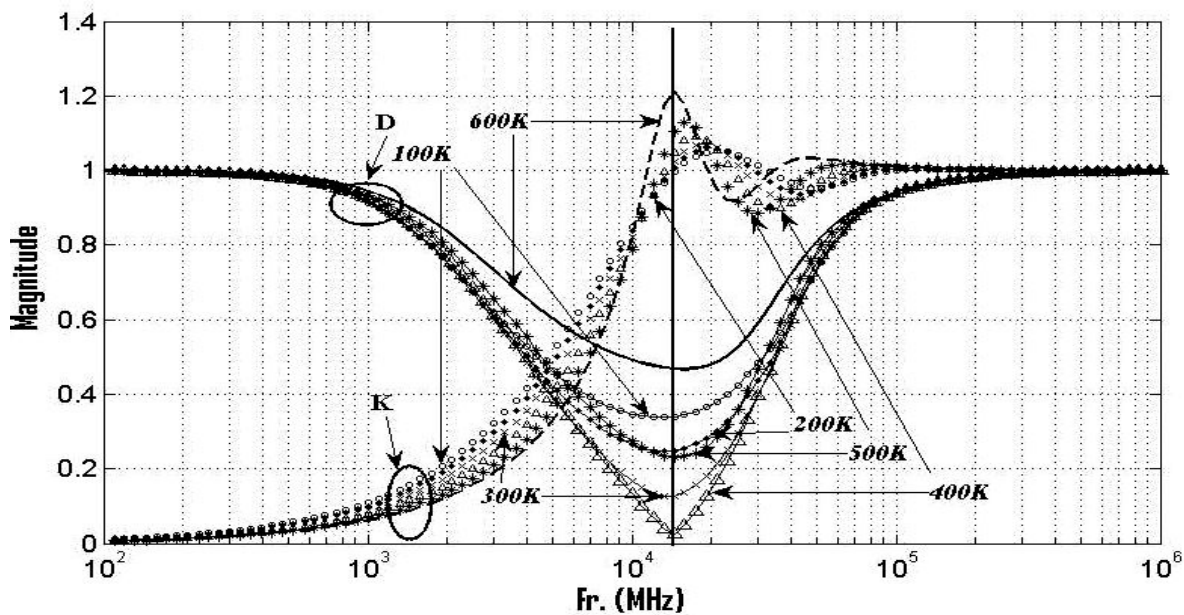


Fig. 2. The relationship between  $\Delta$ - $K$  for HEMT at different temperatures.

Fig. 3 shows the change of  $\Delta$  which affects the Rolletti stability factor with respect to  $S_{11} * S_{22}$  and  $S_{12} * S_{21}$  parameters. The  $S_{11}, S_{12}, S_{21}$  and  $S_{22}$  parameters were obtained from the values of the equivalent circuit of HEMT at 300K. These parameters that effect the  $\Delta$  factor were analyzed in two parts composed of the multiplications a ( $S_{11} * S_{22}$ ) and b ( $S_{12} * S_{21}$ ).

When ( $S_{11} * S_{22} = 1$ ) which corresponds to ( $S_{12} * S_{21} = 0$ ) point, the system is unconditionally unstable. The points ( $S_{12} * S_{21} = 0.28$ ) and ( $S_{11} * S_{22} = 0.16$ ) corresponds to the inflection point. The critical points of the delta values correspond to:

1.  $S_{11} * S_{22} = 0.16, S_{12} * S_{21} = 0.28$  and  $\Delta = 0.12$
2.  $S_{11} * S_{22} = 1, S_{12} * S_{21} = 0$  and  $\Delta = 1$
3.  $S_{11} * S_{22} = 0.52, S_{12} * S_{21} = 0.70$  and  $\Delta = 0.63$ . All these points are the critical pivot points in the operation of HEMT.

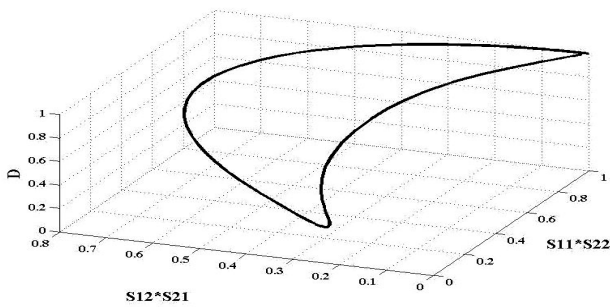


Fig. 3. The change of Delta at 300 K with respect to the scattering parameters.

Fig. 4 shows the relationship between the scattering parameters of HEMT used for the calculation of  $\Delta$  at 300 K. Depending on the scattering variables the  $S_{11} * S_{22} = 0.16, S_{12} * S_{21} = 0.28$  points are the values corresponding to inflection. According to the scattering parameters there is no linearity in the change of  $\Delta$ . Contrary it can be concluded that, there is a high order of non-linearity. In addition to that, there is no linearity in any region among the parameters that affect  $\Delta$  as well.

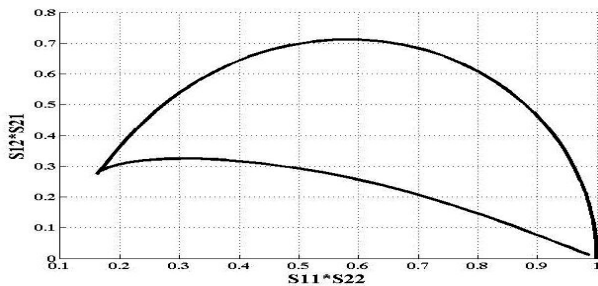


Fig. 4. The relationship between the scattering parameters used to calculate Delta at 300 K.

The change of  $\Delta$  at 300K with respect to  $S_{12} * S_{21}$  is analyzed in Fig. 5. As can be seen in Fig. 5 for  $\Delta = 1$  (D),  $S_{12} * S_{21} = 0$ . Based on this condition HEMT is unconditionally unstable. For the stable condition  $S_{12} * S_{21} = 0.28$  that corresponds to  $\Delta = 0.12$ , HEMT is unconditionally stable.

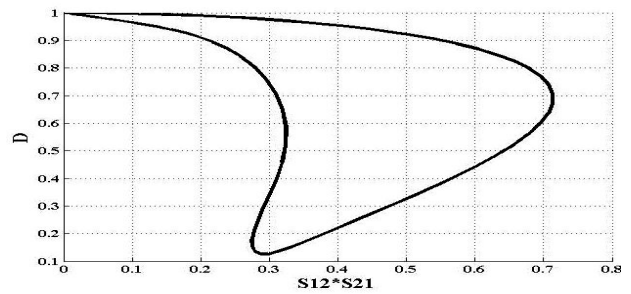


Fig. 5. The change of D (Delta) and  $S_{12} * S_{21}$  at 300 K according to the scattering parameters.

The Figs. 6, 7, 8 and 9 are evaluated together to determine the unconditionally stable and unstable regions of  $\Delta$  (Delta, D) and K.

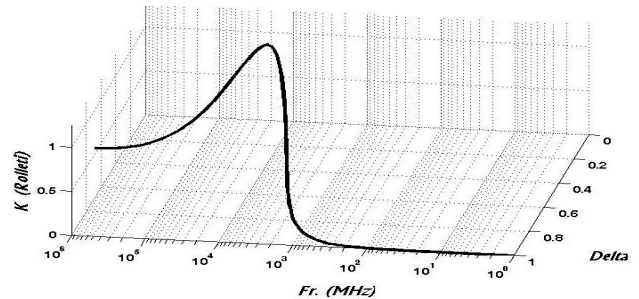


Fig. 6. The change of Rolletti criteria (K), Delta(D) according to frequency at 300 K.

In Fig. 7, 16 GHz point which corresponds to the lowest value of Delta ( $D=0.12$ ) is the best value that HEMT is unconditionally stable.

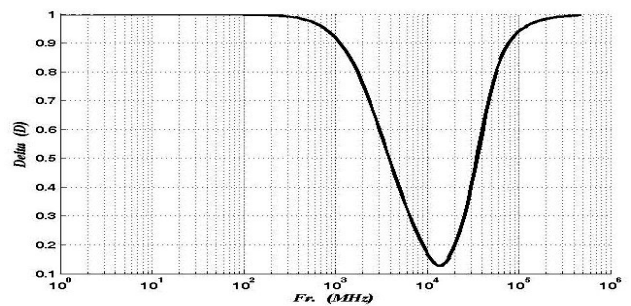


Fig. 7. The change of Delta with frequency at 300 K.

Whereas in Fig. 8, the frequency value at which HEMT is unconditionally stable based on the Rolletti factor is the frequency range from 15 GHz to 25 GHz.

Between 25-75 GHz, it is accepted to be unconditionally unstable and for all frequencies after 75 GHz, it is unconditionally stable. The best frequency for stability is about 19 GHz. At this frequency value, the Rolletti criteria is at its best value ( $K=1.07$ ).

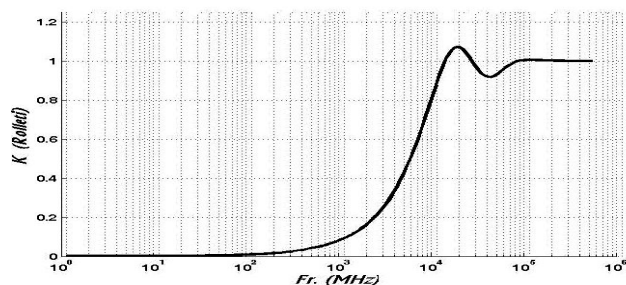


Fig. 8 The change of  $K$  with frequency at 300 K.

Fig. 9 shows the relationship between the Rolletti factor  $K$  and  $\Delta$  when HEMT is at 300 K. The values at which HEMT becomes stable are  $D = 0.9$ ,  $K=1$  and HEMT becomes unconditionally stable. In the range at which HEMT is unconditionally stable  $D$  ranges between  $D=0.12-0.33$ . Here  $K$  suddenly reaches high values and is accepted to be unconditionally stable. The other stability range is the values after  $D = 0.9$ . Here  $K$  values suddenly reach high values again and HEMT is unconditionally accepted to be stable. HEMT operates stably in two regions.

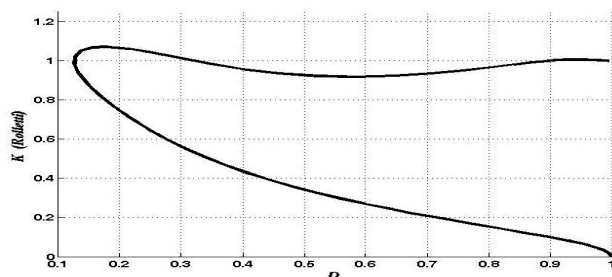


Fig. 9. The relationship between  $K$ - $D$  at 300K.

### 3. Conclusions

The results obtained in this study with respect to the change in temperature can be summarized as follows:

1. As temperature increases, the  $K$  and frequency values become smaller. Also for the highest temperature of 600 K, the oscillation fluctuations reach high values and the steady state frequency interval increases. The probable bandwidth at which HEMT can be used stably becomes smaller.

2. The steady state frequency range is small and the oscillation fluctuations are shorter for the lower temperature value (100K) as well.

3. At a temperature of 400K  $\Delta$  is at its minimum value. The Rolletti stability factor ( $K$ ) becomes lower than 500 K.

4.  $\Delta$  is at its lowest value for all temperatures at 16 GHz. This frequency value is the most sensitive one to the temperature. HEMT is accepted to be working unconditionally stable at this range. On the other hand, the effect of ambient temperature is also very important.

5. It is observed that temperature and change in power are directly related. Also It is clear that as the temperature increases, the power values decrease. Between the two extreme temperatures (100 K - 600 K) a gain difference of 10.8dB is computed. The transducer power difference is found to be 31dB. This value is important for high frequency applications.

6. At the critical temperature of 400K,  $\Delta$  reaches its minimum value whereas it reaches its maximum value at 600K. These two temperature values correspond to the extreme points of HEMT's operating temperature.

7. HEMT operates regionally stable in two regions (Fig. 9).

8. It is determined that the best value of  $\Delta$  for 300K is 0.12 and its frequency is found to be 16 GHz.

9. The best value for the Rolletti stability factor at 300K is determined to be 1.07 and its frequency value is determined to be 19 GHz.

In this study, the most temperature sensitive frequency for HEMT to operate stably is computed as 19 GHz. whereas the best operating temperature is 300 K. Because the voltage gain can be considered to be almost constant up to 1 GHz. Finally, HEMT operates unconditionally stable for frequencies higher than 12GHz. The temperature sensitive variables are the transconductance  $g_m = g_{m1} + g_{m2}v_{gs} + g_{m3}v_{gs}^2$ , output resistance change  $r_{ds} = r_{ds1} + r_{ds2}v_{gs} + r_{ds3}v_{gs}^2$  and gate-source capacitance change  $C_{gs} = C_{gs1} + C_{gs2}v_{gs} + C_{gs3}v_{gs}^2$ . As a result of the change in these variables, the operating characteristics of HEMT change. Therefore HEMT is unconditionally unstable between 140MHz-12GHz according to the Rolletti criteria. Unconditionally stable regions of HEMT depend upon temperature. The best -3 dB bandwidth corresponds to the 300 K value.

### References

- [1] M. Fukuta, Fujitsu Quantum Devices Limited, 2002.
- [2] C. J. Leong, Z. Shen, L. C. Tay, , *Microwave and Optical Technology Letters* **29**(6), 2001.
- [3] A. Tasic, W. A. Serdijn, J. R. Long., Springer, 2006.
- [4] L.T.Wurtz, *IEEE Transactions on Instrumentation and Measurement* **43**(4), 1994.
- [5] G. Crupi, D. M. P. Schreurs, A. Caddemi., *Int. Journal of RF And Micr. Comp.-Aided Eng.*, 417, May 2008.
- [6] M. J. Hwu, Phd Thesis, 1993.
- [7] S. W. Wedge, *IEEE Transactions on Microwave and Techniques* **40**(11), 1992.
- [8] G. Dambrine, A. Cappy, F. Heliodore, E. Playez, *IEEE Trans Micr. Theory Tech.* **36**, 1151 (1988).
- [9] G. Crupi, D. Xiao, D. Schreurs, E. Limiti, A. Caddemi, W. De Raedt, M.Germain, *IEEE Trans*

- Microwave Theory Tech. **54**, 3616 (2006).
- [10] M-Y. Jeon, Microwave and Optical Technology Letters **44**(6), 489 (2005).
- [11] D. M. P. Schreurs, Y. Baeyens, B. K. J. Nauwelaers, W. De Raedt, M. V. Hove, M. V. Rossum, Int. Journal of Micr. And Millimeter-Wave Comp.-Aided Eng. **6**(4), 250 (1996).
- [12] M. Berroth, R. Bosch, IEEE Trans Micr. Theory Tech. **39**, 224 (1991).
- [13] M. Kameche, M. Feham, M. Meliani, N. Benahmet, S. Dali, National Centre of Space Techniques, Algeria Telecom Laboratory, University of Tlemcen, Algeria, 2006.
- [14] R. Tayrani, J. E. Gerber, T. Daniel, R. S. Pengelly, U. L. Rhode, European Micro. Conf, 451, Spain, 1993.
- [15] R. A. Minasian, Electronics Letters **13**(18), 549 (1977).
- [16] S. Yanagawa, H. Ishihara, M. Ohtomo, IEEE Trans Micr. Theory Tech. **44**, 1637 (1996).
- [17] D. S. Chalermwisutkul, Phd Thesis, 2007.
- [18] R. Anholt, S. Swirhun, IEEE Trans Micr. Theory Tech. **39**, 1243 (1991).
- [19] A. H. Jarndal, Ph.D Thesis, 2006.
- [20] A. Miras, E. Legros, IEEE Trans Micr. Theory Tech. **45**, 1018 (1997).
- [21] Q. Z. Liu., Microwave Symposium Digest, 1989.
- [22] M. Garcia, J. Stenarson, H. Zirath, I. Angelov, Microwave and Optical Tech. Letters **16**, 208 (1997).
- [23] A. Jarndal, G. Kompa, IEEE Trans Micr. Theory Tech. **54**, 2949 (2006).
- [24] M. Kameche, M. Feham, Int. Journal of Infrared and Millimeter Waves **27**(5), 687 (2006).
- [25] G. Chen, V. Kumar, R. S. Schwindt, I. Adesida, IEEE Trans Micr. Theory Tech. **54**, 2949 (2006).
- [26] R. W. Anderson, L. Smith, J. Gruszynski, W. Patstone, HP Test-Measurement Application Note 95-1, 1996.
- [27] D. B. Leeson., IEEE 194 RF, 1994.
- [28] A. Ahmed, S. Islam, A. F. M. Anwar, IEEE Trans. On Micr. Theory and Tech. **49**(9), 2001.
- [29] A. Ahmed, S. Islam, A. F. M. Anwar, Solid-State Electronics **47**, 339 (2003).
- [30] Maas, Stephen A., Artech House, Second Edition, 26, 2003.
- [31] J. Golstein, M. Soltan, Microwave Journal **43**, 278 (2000).
- [32] J. M. Rolletti, IRE Transactions Circuit Theory **9**, 29 (1962).
- [33] A. Suarez, R. Quere, Stability Analysis of Nonlinear Microwave Circuits, Artech House, Boston, 2003.
- [34] P. H. Ladbrook, MMIC Design GaAs FET and HEMT, Artech House, Boston, 1989.
- [35] P. Wambacg, W. Sansen, Distortion Analysis of Analog Integrated Circuits, Kluwer Academic Publishers, 2.Ed., Boston, 2001.

---

\*Corresponding author: Fatih.Celebi@eng.ankara.edu.tr